UDC 537.2:621.1



# DEEPLY VIRTUAL COMPTON SCATTERING AND GENERALIZED PARTON DISTRIBUTIONS

**A. FLACHI[1], K. GUDIMA[2], L.L. JENKOVSZKY[3], V. KUVSHINOV[4], V.K. MAGAS[3,5]**

[1]**Universidad Autonoma de Barselona**
*(08193 Bellaterra, Barselona, Spain),*

[2]**Institute of Applied Physics, Acad. of Sci. of Moldova**
*(5, Academy Str., Kishinev, MD-2028, Moldova),*

[3]**Bogolyubov Institute for Theoretical Physics, Nat. Acad. Sci. of Ukraine**
*(14b, Metrolohichna Str., 03143 Kyiv, Ukraine),*

[4]**Institute of Physics, Belarus Nat. Acad. of Sci.**
*(68, F.Skarina Ave., 220072 Minsk, Republik of Belarus),*

[5]**Physics Department, Instituto Superior Tecnico**
*(Rovisco Pais Ave., 1049-001 Lisbon, Portugal)*

An off-mass-shell continuation of the dual model with Mandelstam analyticity is proposed. It can serve as a prototype model for deeply virtual Compton scattering (DVCS) and generalized parton distributions (GPD). With the spin dependence included, the model is fitted to the data on inelastic electron-proton scattering.

## Introduction

DVCS combines the features of inelastic processes with those of an elastic process. The diagram of such a process, $e(k_1)+P_1 \to e'(k_2)+P_2+\gamma(q_2)$, is shown in Fig. 1, where $e(k_1)$, $e'(k_2)$ denote respectively the initial and final electrons of momenta $k_1$, $k_2$, and $P_1$, $P_2$ denote the initial and final momenta of the target, correspondingly.

It has been recently realized [1] that a straightforward generalization of the ordinary parton densities arises in exclusive two-photon processes in the so-called generalized Bjorken region, e.g. in Compton scattering with a highly virtual incoming photon, and in the hard photoproduction of mesons. Here one finds off-forward matrix elements, as distinguished from the forward ones in inclusive reactions.

DVCS is the hard photoproduction of a real photon, i.e. $\gamma^* N \to \gamma N'$. Being a process involving a single hadron, it is one of the cleanest tools to construct GPD, which reduce to ordinary parton distributions in the forward direction. The theoretical efforts and achievements are supported by the experimental results from HERMES, HERA, and CLAS Collaborations, and encouraging future plans.

DVCS is characterized by three independent four-momenta: $P = P_1 + P_2$, $\Delta = P_2 - P_1$, and $q = (q_1+q_2)/2$, where the vectors $P_1$ ($q_1$) and $P_2$ ($q_2$) refer to the incoming and outgoing proton (photon) momentum, respectively.

The conventional Bjorken variable is $x = \frac{Q^2}{2P_1\cdot q_1}$, $Q^2 = -q_1^2$, and $\xi = -\frac{q^2}{q\cdot P}$ is the generalized Bjorken variable. If both photons were virtual, we would have an extra scaling variable $\eta = \frac{\Delta\cdot q}{P\cdot q}$, the skewedness [1, 2]. The reality of the outgoing photon implies the presence of only one scaling variable. Namely, for $q_2^2 = 0$, one has

$$\eta = -\xi\Big(1 + \frac{\Delta^2}{2Q^2}\Big)^{-1}. \qquad (1)$$

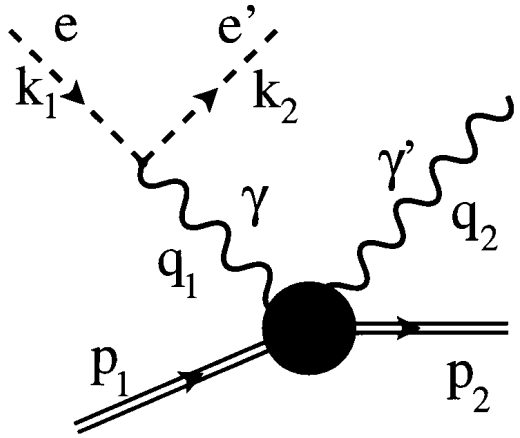


Fig. 1. Kinematics of deeply virtual Compton scattering

The generalized and ordinary Bjorken variables are related by

$$\xi = x\frac{1+\frac{\Delta^2}{2Q^2}}{2-x+x\frac{\Delta^2}{Q^2}}. \qquad (2)$$

Extracting the GPDs from the scattering amplitudes requires to study a number of observables in different reactions, electroproduction of mesons and photons being the main source of information.

Complementarily to ordinary parton distributions, which measure the probability that a quark or gluon carry a fraction of $x$ of the hadron momentum, GPD represents the interference of different wave functions, one where a parton carries the momentum fraction $x+\eta$ and one where this fraction is $x-\eta$, $\eta$ being the skewedness and is fixed in DVCS experiments by external momenta. When $x < \eta$, the GPD should be interpreted as the interference of the wave hadron function with the wave function of the hadron accompanied by a $q\bar{q}$ pair. It is reminiscent of the probability amplitude to extract a meson from a hadron.

Apart from longitudinal momentum fraction variables, GPDs also depend on the squared momentum transfer, $t$, between the initial and final hadrons. A Fourier transform of this transverse momentum information leads to information on the transverse location of quarks and gluons in hadrons [2]. In this way, completely new real-space images of the target can thus be obtained. Quantum photography of the proton, nuclei, and other elementary particles with resolution on the scale of a fraction of femtometer is thus feasible.

Most of the papers on this subject are based on the so-called "handbag" approximation borrowed from DIS, according to which lowest order perturbation theory decouples from hadronic dynamics during the short time of interaction, which is a plausible assumption at large $Q^2$, where perturbative QCD calculations are reliable. However, most of the existing data are accumulated at small and intermediate values of $Q^2$, characterized by large non-perturbative effects. Moreover, the $t$-dependence (at small $t$!) is completely outside the domain of perturbative QCD and is oversimplified in this type of calculations.

Another problem for most of the existing models is the unknown relative phase of the DVCS amplitude. Experimentally, it can, in principle, be extracted from the interference between the DVCS and Bethe-Heitler amplitudes, similar to the case of the Coulomb interference in the forward cone of elastic hadron scattering. Theoretically, this phase can be approximately reconstructed by means of the dispersion relations or their simplified version of the derivative dispersion relations, as it was done in [3].

The virtue of the present approach based on a Regge-pole model is the presence in the scattering amplitude of $t$-dependence and of the phase as well as its explicit energy dependence compatible with unitarity. At high energies, the contribution of a dipole pomeron [5] dominates, while subleading contributions (secondary reggeons) and spin effects become important at moderate and low energies (for a recent treatment of the problem see [6]). The dipole pomeron has many successful applications — both in elastic hadron scattering, DIS (virtual forward Compton scattering) as well as in photoproduction of vector mesons [5]. Recently it was extended to electroproduction of vector mesons [7]. In this paper, we apply this extension to electroproduction of real photons at HERA and elsewhere.

In [11—13], it was suggested to use dual amplitudes with Mandelstam analyticity (DAMA) as a model for GPD in general and for DVCS in particular. We recall that DAMA realizes the duality between direct-channel resonances and high-energy Regge behavior ("Veneziano-duality"). By introducing $Q^2$-dependence in DAMA, we have extended the model off mass shell and have shown [11, 12] how the parton-hadron (or "Bloom-Gilman") duality is realized in this way. With the above specification, DAMA can serve as an explicit model valid for all values of the Mandelstam variables $s$, $t$, and $u$ as well as any $Q^2$, thus realizing the ideas of DVCS and related GPDs.

We start with inclusive electron-nucleon scattering shown in Fig. 2, both at high energies, typical of HERA, and low energies, with the JLab data in mind (see [13] for more details).

The complex pattern of the nucleon structure function in the resonance region was developed long time ago (see, for example [14]). There are several dozens of resonances in the $\gamma^* p$ system in the region above the pion-nucleon threshold, but only a few of them can be identified more or less unambiguously for various reasons. Therefore, instead of identifying each resonance, one considers a few maxima above the elastic scattering peak, corresponding to some "effective" resonance contributions. Recent results from the JLab [8, 9] renewed the interest in the subject and they call for a more detailed phenomenological analysis of the data and a better understanding of the underlying dynamics. The basic idea in our approach is the use the off-mass-shell continuation of the dual amplitude with nonlinear complex Regge trajectories.

We adopt the two-component picture of strong interactions, according to which direct-channel resonances are dual to cross-channel Regge exchanges and the smooth background in the $s$-channel is dual to the Pomeron exchange in the $t$-channel. As explained in [11], the background corresponds in the dual model to a pole term with exotic trajectory that does not produce any resonance.

We study inclusive electron-nucleon scattering in which the central object of study is the nucleon structure function (SF) uniquely related to the photoproduction cross section by

$$F_2(x,Q^2) = \frac{Q^2(1-x)}{4\pi\alpha(1+4m^2x^2/Q^2)}\sigma_t^{\gamma^* p}, \tag{3}$$

where the total cross section (including by unitarity all possible intermediate states allowed by energy and quantum number conservation), $\sigma_t^{\gamma^* p}$, is the imaginary part of the forward Compton scattering amplitude, $A(s,Q^2)$,

$$\sigma_t^{\gamma^* p}(s) = \mathcal{I}m\ A(s,Q^2)\ . \tag{4}$$

The center of mass energy of the $\gamma^* p$ system, the negative squared photon virtuality $Q^2$, and the Bjorken variable $x$ are related by

$$s = W^2 = Q^2(1-x)/x + m^2. \tag{5}$$

Most, if not all of the two dozens (almost) certain resonances contribute, with different weights, to the $\gamma^* N$ total cross section or to the nucleon SF. It is clear that a systematic account for all these resonances (plus those to be confirmed) is not an easy task. A much more economic way to fully account for all possible intermediate states in the resonance region is in terms of the $s$-channel

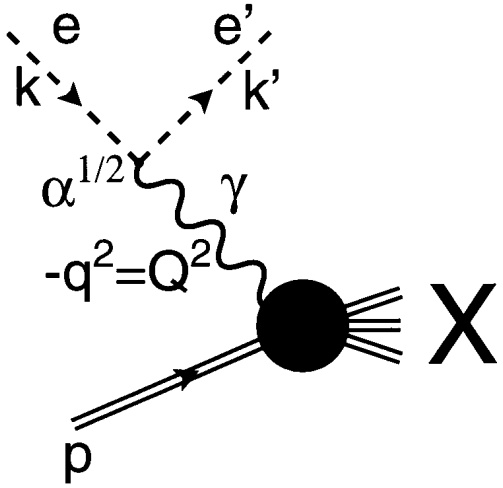


Fig. 2. Kinematics of deep inelastic scattering

Regge trajectories, which automatically include the huge number of resonances as recurrences, appearing on the trajectories. Also, by generalizing the concept of a resonance (a Regge trajectory realizes the analytic continuation of the discrete resonance spin and is an indispensable ingredient of dual models!), the trajectory may also be used to classify the resonances by eliminating some candidates and predicting others. The above mentioned resonances lie on several trajectories: positive- and negative-parity $N^*$ and $\Delta$ trajectories.

We use Regge trajectories with a threshold singularity and nonvanishing imaginary part in the form:

$$\alpha(s) = \alpha_0 + \alpha_1 s + \alpha_2(\sqrt{s_0} - \sqrt{s_0 - s}), \tag{6}$$

where $s_0$ is the lightest threshold, $s_0 = (m_\pi + m_p)^2 = 1.14\ \mathrm{GeV}^2$ in our case [11—13, 19].

We take the exotic trajectory as

$$\alpha_E(s) = \alpha_E(0) + \alpha_{1E}(\sqrt{s_E} - \sqrt{s_E - s}), \tag{7}$$

where the intercept $\alpha_E(0)$, $\alpha_{1E}$, and the effective exotic threshold $s_E$ are free parameters. As the first approximation, we can assume the following expression for the exotic trajectory [11]:

$$\alpha_E(s) = 0.5 + 0.12(\sqrt{s_E} - \sqrt{s_E - s})\ , \tag{8}$$

where $s_E = 1.311\ \mathrm{GeV}^2$.

## 1. The Model

We present the form factors as sums of three terms [18, 20]: $G_+(Q^2)$, $G_0(Q^2)$ and $G_-(Q^2)$, corresponding

to $\gamma^* N \to R$ helicity transition amplitudes in the rest frame of the resonance $R$:

$$G_{\lambda_\gamma} = \frac{\langle R, \lambda_R = \lambda_N - \lambda_\gamma | J(0) | N, \lambda_N \rangle}{m}, \tag{9}$$

where $\lambda_R, \lambda_N$, and $\lambda_\gamma$ are the resonance, nucleon and photon helicities, $J(0)$ is the current operator; $\lambda_\gamma$ assumes the values $-1, 0$ and $+1$. Correspondingly, the squared form factor [13] is given by a sum

$$|G_+(Q^2)|^2 + 2|G_0(Q^2)|^2 + |G_-(Q^2)|^2. \tag{10}$$

The explicit form of these form factors is known only near their thresholds $|\vec{q}| \to 0$, while their large-$Q^2$ behavior may be constrained by the quark counting rules.

According to [21], near the threshold, one has

$$G_\pm(Q^2) \sim |\vec{q}|^{J-3/2}, \quad G_0(Q^2) \sim \frac{q_0}{|\vec{q}|} |\vec{q}|^{J-1/2} \tag{11}$$

for the so-called normal $(1/2^+ \to 3/2^-, 5/2^+, 7/2^-, ...)$ transitions and

$$G_\pm(Q^2 \sim |\vec{q}|^{J-1/2}, \quad G_0(Q^2) \sim \frac{q_0}{|\vec{q}|} |\vec{q}|^{J+1/2} \tag{12}$$

for the anomalous $(1/2^+ \to 1/2^-, \ 3/2^+, 5/2^-, ...)$ transitions, where

$$|\vec{q}| = \frac{\sqrt{(M^2 - m^2 - Q^2)^2 + 4M^2 Q^2}}{2M}, \tag{13}$$

$$q_0 = \frac{M^2 - m^2 - Q^2}{2M}, \tag{14}$$

$M$ is a resonance mass.

Following the quark counting rules, in [20] (for a recent treatment, see [18]), the large-$Q^2$ behavior of $G$'s was assumed to be

$$G_+ \sim Q^{-3}, \ G_0 \sim Q^{-4}, \ G_- \sim Q^{-5}. \tag{15}$$

Let us note that while this is reasonable (modulo logarithmic factors) for elastic form factors, it may not be true any more for inelastic (transition) form factors. For example, dual models (see Eq. (1) and [11]) predict powers of the form factors to increase with increasing excitation (resonance spin). This discrepancy can be resolved only experimentally, although a model-independent analysis of the $Q^2$-dependence for various nuclear excitations is biased by the (unknown) background.

In [18], the following expressions for the $G$'s, combining the above threshold- (11), (12) with the asymptotic behavior (15), was suggested:

$$|G_\pm|^2 = |G_\pm(0)|^2 \times$$

$$\times \left( \frac{|\vec{q}|}{|\vec{q}|_{Q=0}} \frac{Q_0'^2}{Q^2 + Q_0'^2} \right)^{2J-3} \left( \frac{Q_0'^2}{Q^2 + Q_0'^2} \right)^{m_\pm}, \tag{16}$$

$$|G_0|^2 = C^2 \left( \frac{Q_0^2}{Q^2 + Q_0^2} \right)^{2a} \frac{q_0^2}{|\vec{q}|^2} \times$$

$$\times \left( \frac{|\vec{q}|}{|\vec{q}|_{Q=0}} \frac{Q_0'^2}{Q^2 + Q_0'^2} \right)^{2J-1} \left( \frac{Q_0^2}{Q^2 + Q_0^2} \right)^{m_0} \tag{17}$$

for the normal transitions and

$$|G_\pm|^2 = |G_\pm(0)|^2 \times$$

$$\times \left( \frac{|\vec{q}|}{|\vec{q}|_{Q=0}} \frac{Q_0'^2}{Q^2 + Q_0'^2} \right)^{2J-1} \left( \frac{Q_0'^2}{Q^2 + Q_0'^2} \right)^{m_\pm}, \tag{18}$$

$$|G_0|^2 = C^2 \left( \frac{Q_0^2}{Q^2 + Q_0^2} \right)^{2a} \times$$

$$\times \left( \frac{q_0^2}{|\vec{q}|^2} \frac{Q_0'^2}{Q^2 + Q_0'^2} \right)^{2J+1} \left( \frac{Q_0^2}{Q^2 + Q_0^2} \right)^{m_0} \tag{19}$$

for the anomalous ones, where $m_+ = 3$, $m_0 = 4$, $m_- = 5$ count the quarks, $C$ and $a$ are free parameters. The form factors at $Q^2 = 0$ are related to the known (measurable) helicity photoproduction amplitudes $A_{1/2}$ and $A_{3/2}$ by

$$|G_{+,-}(0)| = \frac{1}{\sqrt{4\pi\alpha}} \sqrt{\frac{M}{M - m}} |A_{1/2,3/2}|. \tag{20}$$

The values of the helicity amplitudes are quoted by experimentalists [15] (those relevant to the present discussion are compiled also in [18]).

## 2. Comparison with Data

We have fitted the above model to the JLab data [8, 9] by keeping the contribution from three prominent resonances, namely $\Delta(1232)$, $N^*(1520)$ and $N^*(1680)$, i.e. we have used only three baryon trajectories with one resonance on each (for more details, see [19] and references therein).

As argued in [11], only a limited number of resonances appears on the trajectories, i.e. their real part is bounded. For practical reasons, we have replaced the formal condition $\mathcal{R}e\ \alpha(s) < \text{const}$ by a finite sum (actually this sum has only one term in our case),

introducing a linear term in the baryon trajectory to approximate the contribution from heavy thresholds (see Eq. (6)).

Since, by definition, the smooth background does not show any resonance, here we keep also only one term in the corresponding sum.

For the sake of simplicity, we also neglected the cross term containing $G_0$ (and the coefficient $C$), since it is small relative to the other two terms in Eq. (10) [18].

To be specific, we write explicitly three resonance terms to be fitted to the data:

$$\mathcal{I}m\ A(s,Q^2) = \text{norm}\times$$

$$\times\left[\frac{f_\Delta I_\Delta}{(1-R_\Delta)^2+I_\Delta^2}+\frac{f_{N^-}I_{N^-}}{(1-R_{N^-})^2+I_{N^-}^2}+\right. \tag{21}$$

$$\left.+\frac{f_{N^+}I_{N^+}}{(2-R_{N^+})^2+I_{N^+}^2}+\text{background}\right],$$

where, e.g., $f_\Delta$ is calculated according to Eqs. (10), (16), (18):

$$f_\Delta = \left(\frac{|\vec{q}|}{|\vec{q}|_{Q=0}}\frac{Q_0'^2}{Q^2+Q_0'^2}\right)^{2J-1=2}\times$$

$$\times\left(|G_+(0)|^2\left(\frac{Q_0^2}{Q^2+Q_0^2}\right)^3+|G_-(0)|^2\left(\frac{Q_0^2}{Q^2+Q_0^2}\right)^5\right); \tag{22}$$

$R$ and $I$ denote the real and imaginary parts of the relevant trajectory specified by the subscript. Similar expressions can be easily cast for $f_{N^+}$ and for $f_{N^-}$ as well.

The background is modeled in the following way [19]:

$$\text{background} = \frac{f_E I_E}{(n_E^{\min}-R_E)^2+I_E^2}, \tag{23}$$

$$f_E = G_E\left(\frac{Q_E^2}{Q^2+Q_E^2}\right)^4. \tag{24}$$

The form factors at $Q^2=0$ can be simply calculated from Eq. (20) by inserting in the known [15] (see also Table 1 in [18]) values of the relevant photoproduction amplitudes, $\text{GeV}^{-1/2}$:

$$A_{\Delta(1232)}(1/2,3/2) = (-0.141,\ -0.258);$$

$$A_{N(1520))}(1/2,3/2) = (-0.022,\ 0.167);$$

$$A_{N(1680)}(1/2,3/2) = (-0.017,\ 0.127).$$

The resulting fit to the SLAC and JLab data is presented in Table. The fit is not so good ($\chi^2_{\text{d.o.f.}} = 9.4$), but we would like to stress that this is actually only the first rough fit over the new dataset without any preselection. What was done is actually the following. In [19], we have performed fit with the same parameterization over the 662 preselected (see Ref. [13] for details) points from [8]. For new fit presented here, we have added to the above points the complete dataset from [9], which is actually much bigger — 4191 points. The work is still in progress and we are planning to come up with better fit.

## Conclusions

We started from idea that deep inelastic scattering can be described by a sum of direct channel resonances lying on Regge trajectories. The form of these trajectories is crucial for the dynamics. It is constrained by analyticity, unitarity, and by the experimental data. The dual model includes the spin and helicity structure of the amplitudes as well as its threshold behavior.

The important step performed in our work after [18] is the "Reggization" of the Breit—Wigner pole terms (21), i.e. single resonance terms in [18] are replaced by those including relevant baryon trajectories. The form of these trajectories, constrained by analyticity, unitarity, and by the experimental data is crucial for the dynamics. The use of baryon trajectories instead of individual

**The parameters of the fit**

| | | |
|---|---|---|
| $N_1^*$ | $\alpha_0$ | −0.8377 (fixed)$^\diamond$ |
| | $\alpha_1$ | 0.9620 |
| | $\alpha_2$ | 0.1673 |
| $N_2^*$ | $\alpha_0$ | −0.37(fixed)$^\diamond$ |
| | $\alpha_1$ | 0.9806 |
| | $\alpha_2$ | 0.0741 |
| $\Delta$ | $\alpha_0$ | 0.0038 (fixed)$^\diamond$ |
| | $\alpha_1$ | 0.8910 |
| | $\alpha_2$ | 0.1529 |
| | $s_0$, GeV$^2$ | 1.14 (fixed)$^\diamond$ |
| $E$ | $\alpha_0$ | 0.1019 |
| | $\alpha_2$ | 0.3372 |
| | $s_E$, GeV$^2$ | 1.3085 |
| | $G_{\text{exot}}$ | 3.6980 |
| | $Q^2_{\text{exot}}$, GeV$^2$ | 4.6006 |
| | $Q_0^2$ | 2.5000 |
| | $Q_0'^2$ | 0.4058 |
| | norm | 0.0674 |
| | $\chi^2_{\text{d.o.f.}}$ | 9.4036 |

N o t e. $^\diamond$ Using intercepts and thresholds as free parameters do not improve the fit, but intercepts may get values far from original.

resonances not only makes the model economical (several resonances are replaced by one trajectory) but also helps in classifying the resonances, by including the "right" ones and eliminating those nonexistent.

To fix the ideas and to make a rough fit to the data, we constructed a simplified model with just 3 baryon trajectories, in which heavy thresholds have been replaced for simpicity by a linear term, and with the lowest-lying resonances. In fact, apart from the "prominent" three resonances, many more should be included by means of relevant baryon trajectories. To this end, an independent study of baryon trajectories and updated fits to dozens of existing resonances should be done. We intend to continue working in this direction.

L.J. and V.M. acknowledge the support by INTAS, Grant 00-00366.

1. *Müller D. et al.*// Fotschr. Phys. **42** (1994) 101; *Ji X.*// Phys. Rev. Lett. **78** (1997) 610; *Radyushkin A.V.*//Phys. Rev. **D56** (1997) 5524; *Diehl M. et al.*// Phys. Lett. **B411** (1997) 193; *Blümlein J., Geyer B., Robaschik D.*// Nucl. Phys. **B560** (1999) 283; *Belitsky A.V., Müller D., Kirschner A.*// Nucl. Phys. **B629** (2002) 323; *Guichon P.A.M., Vanderhaeghen M.*// Prog. Part. Nucl. Phys. **41** (1998) 125.
2. *Ralston J.P., Pire B.*// hep-ph/0110075; *Pire B.*// hep-ph/0211093.
3. *Frankfurt L.L., Freund A., Strickman M.*// Phys. Lett. **B460** (1999) 417; *Frankfurt L.L., Freund A., Strickman M.*// Phys. Rev. **D58** (1998) 114001; **D59** (1999) 119901.
4. *Fiore R., Jenkovszky L.L., Paccanoni F., Papa A.*// Phys. Rev. **D65** (2002) 077505.
5. *Jenkovszky L.L., Martynov E.S., Paccanoni F.*// hep-ph/9608384; *Fiore R., Jenkovszky L.L., Paccanoni F.*// Europ. Phys. J. **C10** (1999) 461; *Martynov E., Predazzi E., Prokudin A.*//Ibid. **C26** (2002) 271; hep-ph/0211430.
6. *Favart L., Machado M.V.T.*// hep-ph/0302079 and DESY 03-016.
7. *Fiore R., Jenkovszky L.L., Paccanoni F., Prokudin A.*// hep-ph/0302195.
8. *Niculescu I. et al.*// Phys. Rev. Lett. **85** (2000) 1182; 1186.
9. *Osipenko M. et al.*// CLAS-NOTE-2003-001, (2003).
10. *Elouadrhirs L.*// hep-ph/0210341.
11. *Jenkovszky L.L., Magas V.K., Predazzi E.*// Europ. Phys. J. **A12** (2001) 361.
12. *Jenkovszky L.L., Magas V.K., Predazzi E.*// nucl-th/0110085; *Jenkovszky L.L., Magas V.K.*// hep-ph/0111398; *Jenkovszky L.L. et al.* //Proc. on New Trend in High-Energy Physics, Yalta, Crimea, Ukraine, Sept. 22—29, 2001/ ed. by P.N. Bogolyubov and L.L. Jenkovszky (BITP, Kiev, 2001).— P. 178.
13. *Fiore R. et al.*// Europ. Phys. J. **A15** (2002) 505.
14. *Stein S. et al.*// Phys. Rev. **12** (1975) 1884.
15. *Hagiwara K. et al.*// Phys. Rev. **D66** 010001 (2002).
16. *Introduction* to Quarks and Partons. — New York: Academic Press, 1978.
17. *Close F.E., Isgur N.*// Phys. Lett. **B509** (2001) 81.
18. *Davydovsky V.V., Struminsky B.V.*// hep-ph/0205130.
19. *Fiore R. et al.*// hep-ph/0212030; *Jenkovszky L.L., Magas V.K.*// Proc. XXXVI Annual Winter School on Nuclear and Particle Physics, St.-Petersburg, Russia, 25 Feb. — 3 Mar., 2002 (in press); Proc. 12th Intern. Seminar on High Energy Physics Quarks'2002, Novgorod, Russia, June 1—7, 2002 (in press); *Jenkovszky L.L. et al.*// Proc. Third Bolyai—Gauss—Lobachevsky Conf. "Non-Euclidean Geometry in Modern Physics", Tirgu—Mures—Marosvasarhely, Transilvania, Romania, July 3—6, 2002 (in press).
20. *Carlson C.E., Mukhopadhyay N.C.*// Phys. Rev. Lett. **74** (1995) 1288; Phys. Rev. **D58** (1998) 094029.
21. *Bjorken J.D., Walecka J.D.*// Ann. Phys. **38** (1966) 35.

Received 29.04.03

## ГЛИБОКОНЕПРУЖНЕ КОМПТОНІВСЬКЕ РОЗСІЯННЯ ТА УЗАГАЛЬНЕНІ ПАРТОННІ РОЗПОДІЛИ

*А. Флакі, К. Гудіма, Л. Єнковський, В. Кувшинов, В. Магас*

Р е з ю м е

Запропоновано можливість подовження дуальної амплітуди з мандельштамівською аналітичністю за масову поверхню. Така амплітуда може служити як модель глибоконепружного комптонівського розсіяння та узагальнених партонних розподілів. Після включення до моделі спінової залежності проведено порівняння з експериментальними даними про непружне розсіяння електронів на протонах.

## ГЛУБОКОНЕУПРУГОЕ КОМПТОНОВСКОЕ РАССЕЯНИЕ И ОБОБЩЕННЫЕ ПАРТОННЫЕ РАСПРЕДЕЛЕНИЯ

*А. Флаки, К. Гудима, Л. Енковский, В. Кувшинов, В. Магас*

Р е з ю м е

Предложен путь выхода дуальной амплитуды с мандельштамовской аналитичностью за массовую поверхность. Такая амплитуда может служить моделью глубоконеупругого комптоновского рассеяния и обобщенных партонных распределений. С учетом спиновой зависимости выполнено сравнение с экспериментальными данными о неупругом рассеянии электронов на протонах.